Microwave response due to light-induced changes in the complex dielectric constant of semiconductors

Serguei Grabtchak and Michael Cocivera
Guelph-Waterloo Centre for Graduate Work in Chemistry, University of Guelph, Guelph, Ontario, Canada N1G 2W1
(Received 22 September 1997; revised manuscript received 20 April 1998)

Cavity perturbation theory was extended to account for light-induced changes in the complex dielectric constant, as a second perturbation, and the equations were used to interpret the microwave response in the advanced method of transient microwave photoconductivity (AMTMP). The equations obtained earlier from a simpler, first cavity perturbation theory, and those derived for simple geometries are shown to be special cases of this more general theory. For AMTMP, the harmonic-oscillator model can account for the changes in the real and imaginary parts of the dielectric constant made by free and trapped electrons, including plasma effects. The decay of the photoconductivity in semi-insulating (SI) GaAs is dominated by changes in the concentration of electrons, and changes in the mobility can be neglected. The difference between CdSe and SI GaAs in regard to changes in the real part of the dielectric constant is due to the substantially larger mobility in SI GaAs. [S0163-1829(98)10231-X]

I. INTRODUCTION

Photoconductivity studies of semi-insulating (SI) gallium arsenide go back to early works of Bube.[1] In spite of many papers on this subject,[2–10] photoelectronic properties of single-crystal SI GaAs are still not fully understood. Due to autocompensation[11] undoped SI GaAs possesses many sub-band gap states[12] to cause carrier dynamics similar to that found in polycrystalline materials. The present study of SI GaAs employed the advanced method of transient microwave photoconductivity (AMTMP), which involved measurement of time-dependent changes in the real and imaginary parts of the complex dielectric constant.[7–10] Transient microwave photoconductivity (TMP), a popular method to study photoeffects of semiconductors, is sensitive only to conduction electrons. As a result, AMTMP was developed to extend TMP to include the determination of the photodielectric effect.[13–15] The essential feature of this method is the simultaneous determination of cavity quality factor changes $\delta(1/2Q_L)$ (''photoconductive effect'') and the shift of the resonance frequency δf_0 (''photodielectric effect''), which can be related to free (conduction band) and trapped electrons, respectively. This method has been used to study CdSe films and single crystals of Si.[13–17]

Insertion of a semiconductor or dielectric material into a microwave cavity causes a change in the resonance frequency f_0 and the cavity quality factor Q_L. Slater[18] used cavity perturbation theory to relate these changes to real and imaginary parts of the complex dielectric constant $\varepsilon^*=\varepsilon'-j\varepsilon''$ for various materials. This first perturbation applies to a sample placed in an *empty* cavity, and it was used to determine absolute values of the real and the imaginary parts of the dielectric constant.[19–26] This treatment cannot be applied to AMTMP because the sample is already in the cavity and light is used to produce excess electrons. This second perturbation causes a *change* in the complex dielectric constant $\delta\varepsilon^*=\delta\varepsilon'-j\delta\varepsilon''$. In this paper, general equations are derived for this second perturbation.

Irradiation creates excess carriers in an active volume of the sample, which is not necessarily equal to the total volume. In addition to size, the geometry of this active volume determines the exact form of the final expressions for $\delta\varepsilon'$ and for $\delta\varepsilon''$, and these expressions are known for only a limited number of sample geometries.[19] Previously[13–15] we used a long thin strip approximation for the sample geometry, but this approximation restricts the samples that can be studied by AMTMP. In this paper, general perturbation expressions are developed using a depolarization factor L to include the dependence on the sample geometry. As well, the harmonic-oscillator model is used to relate AMTMP results with quantitative and qualitative changes in the complex dielectric constant. For SI GaAs, the AMTMP results were dominated by changes in the electron concentration, and changes in the mobility had a minor effect.

II. SECOND CAVITY PERTURBATION

The change in the complex angular frequency ω_2^* for a nonmagnetic sample is[18]

$$\frac{\delta\omega^*}{\omega_2^*}=-\frac{(\varepsilon_2^*-\varepsilon_1^*)\int_{V_s}\bar{F}_1\bar{F}_2dV}{2\varepsilon_{\text{medium}}^*\int_{V_c-V_s}\bar{F}_1\bar{F}_2dV+2\varepsilon_1^*\int_{V_s}\bar{F}_1\bar{F}_2dV},\tag{1}$$

in which ε_1^* and ε_2^* are the complex dielectric constants of the sample before and after illumination, V_s and V_c are the active sample and cavity volumes, and $\bar{F}$ is the electric-field vector. Note that F_1 and F_2 correspond to the field in the sample before and after illumination. The first integration in the denominator is over the cavity volume and includes $\varepsilon_{\text{medium}}^*$, the dielectric constant of the medium filling the cavity. Normally, the experiments are done in the air or in vacuum, so the dielectric constant equals 1. When the sample is sufficiently small and does not change significantly, the field in the cavity volume, $F_2=F_1=F_0$ is a good approximation, and F_0 is the field in the cavity outside the sample.

 © 1998 The American Physical Society

Changes in the resonance frequency f_0 and loaded cavity quality factor Q_L also can be related to the changes in the complex angular frequency by[21]

$$\frac{\delta\omega^*}{\omega_2^*}=\frac{\delta f_0}{f_{02}}+j\delta\left(\frac{1}{2Q_L}\right), \tag{2}$$

in which $\delta f_0=f_{02}-f_{01}$ and $\delta(1/2Q_L)=(1/2Q_{L2})-(1/2Q_{L1})$. The cavity quality factor is

$$Q_L=f_0/\Delta f_{1/2}, \tag{3}$$

in which $\Delta f_{1/2}$ is the full bandwidth at half maximum of the reflected power.

Equating Eqs. (1) and (2) when $F_2=F_1=F_0$ one obtains the simplest expression for low conductivity samples:

$$\delta\varepsilon'=-\frac{1}{2}\frac{V_c\delta f_0}{V_s f_{20}}\equiv-\frac{\delta f_0}{f_{20}G},$$
$$\delta\varepsilon''=\frac{1}{4}\frac{V_c\delta(\Delta f_{1/2})}{V_s f_{20}}\equiv\frac{\delta(\Delta f_{1/2})}{2f_{20}G}. \tag{4}$$

These equations are almost the same as those derived previously[13] except ε_1' is absent. Therefore, changes in the complex dielectric constant were overestimated previously.[13]

For the general case in which the first term dominates in the denominator, the field F_2 inside the sample can be related to the external field F_0 using[27] a depolarization factor L_2:

$$F_2=\frac{F_0}{1+L_2(\varepsilon_2^*-1)}, \tag{5}$$

which is valid when a sample with dielectric constant ε_2^* is placed in a vacuum. An analogous expression applies to the field F_1. The same equations were used to derive the corresponding relations for the *first* perturbation.[23] For the second perturbation, substitution in the numerator and integration for a rectangular TE_{101} cavity gives

$$\frac{\delta\omega^*}{\omega_2^*}=-(\varepsilon_2^*-\varepsilon_1^*)G\,\frac{1}{1+L_2(\varepsilon_2^*-1)}\,\frac{1}{1+L_1(\varepsilon_1^*-1)}, \tag{6}$$

in which $G=2V_S/V_C$. The simplest solution is obtained when the whole sample is illuminated, and then $L_2=L_1=L$.

Equating Eq. (2) to Eq. (6) and separating the real and the imaginary parts provides a system of two equations for changes in the real and imaginary parts of the dielectric constant. MAPLE V was used to solve this system *analytically* to give general equations that are too complicated for publication. However, suitable constants can be chosen to reduce them to the forms derived earlier for simpler models. For example, first perturbation expressions can be considered as a special case and can be obtained by using $\varepsilon_1^*=1$ and $\varepsilon_2^*=\varepsilon'-j\varepsilon''$ (using the relative dielectric constant). The resulting expressions are identical to those derived earlier except that the frequency shift was defined to be positive.[23] In addition, the general second perturbation equations can be used to obtain any of the approximate relations derived earlier for various sample geometries by setting L to the appropriate values.[28]

For many practical cases, $L=0$ may not be a good approximation. For thin films and thin strips of wafers it is more appropriate to use the depolarization factor developed for a general ellipsoid:[29]

$$L=\frac{bc}{l^2}\left[\ln\left(\frac{4l}{b+c}\right)-1\right], \tag{7}$$

in which b, c, l are the semiaxes of the ellipsoid. For the SI GaAs sample used in our experiments (5 mm long, ≈1.5 mm wide, 0.52 mm thick), L obtained from Eq. (7) was sufficiently small (0.007) so that solutions of Eq. (6) gave $\delta\varepsilon'$ and $\delta\varepsilon''$ nearly identical to the values obtained for $L=0$. In other words for the sample dimensions used, the approximation of an infinitely long thin strip is justified.

In view of the strong dependence of L on geometry, it is not surprising that sample orientation relative to the microwave field affects photoconductivity measurements. Anisotropy was observed when the field was parallel or perpendicular to thin flat microcrystals in T-grain emulsions.[20]

III. HARMONIC-OSCILLATOR MODEL

A simple physical model of dynamic dielectric polarization treats the motion of electrons in the microwave field as harmonic oscillation.[21,30] Benedict and Shockley[31] used this model to determine the effective mass of free electrons in germanium. Recent work[32] showed that this model adequately reproduces the dielectric constant of a semiconductor for excitation levels up to 10^{20} cm^{-3}. In the context of AMTMP, this model provides an adequate description of free and trapped electrons including plasma effects.

A. Free electron effects

According to the Drude-Zener theory, the free-carrier effects on the real and imaginary parts of the dielectric constant are

$$\delta\varepsilon'_{\text{free}}(t)=-\Delta n(t)e^2\tau^2/\varepsilon_0 m^*[1+(\omega\tau)^2], \tag{8}$$

$$\delta\varepsilon''_{\text{free}}(t)=\Delta n(t)e^2\tau/\omega\varepsilon_0 m^*[1+(\omega\tau)^2], \tag{9}$$

in which $\Delta n(t)$ is the change in the volume concentration of free carriers, m^* is the effective mass, τ is the momentum relaxation time, and ω the microwave angular frequency. The momentum relaxation time becomes time dependent when the carrier mobility μ varies with time:

$$\tau(t)=m^*[\mu_0+\Delta\mu(t)]/e. \tag{10}$$

In this equation μ_0 is the ''dark'' equilibrium mobility and $\Delta\mu(t)$ is the change in the mobility value after excitation. From Eq. (8) one can see that conduction-band electrons cause a negative change in the real part of the dielectric constant. Because the frequency is very nearly constant during AMTMP measurements, it is informative to analyze Eqs. (8) and (9) for various mobility values keeping the frequency constant. In Fig. 1, $-\delta\varepsilon'$ and $\delta\varepsilon''$ are plotted as a function

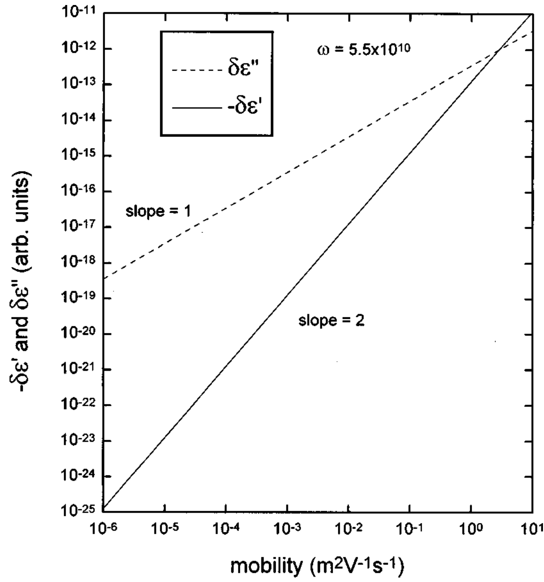

FIG. 1. Changes in the real and imaginary parts of the complex dielectric constant due to excess free electrons as functions of mobility.

of the mobility for an angular frequency corresponding to microwave measurements (5.5×10^{10} rad/s). The values have been scaled to permit comparison of the plots. Thus, the change in the imaginary part is positive and proportional to the first power of the mobility, whereas the change in the real part of the dielectric constant is negative and proportional to the square of the mobility. In Sec. IV this behavior is discussed in regard to the experimental results for low-mobility ($\sim10^{-3}$ m^2/V s) CdSe thin film and high-mobility (~1 m^2/V s) single-crystal SI GaAs.

B. Plasma effects

Plasma depolarization occurs when the concentration of excess carriers is sufficiently large to cause a harmonic restoring force due to confinement of mobile carriers in a small sample volume.[30] Including this force in the equation of motion and using the relations between the complex dielectric constant and the complex conductivity gives[30]

$$\delta\varepsilon'_{\rm plasm}(t)=-\Delta n(t)e^2\tau^2(1-\omega_P^2/\omega^2)/\varepsilon_0 m^* \times[1+\{(1-\omega_P^2/\omega^2)\omega\tau\}^2], \tag{11}$$

$$\delta\varepsilon''_{\rm plasm}(t)=\Delta n(t)e^2\tau/\varepsilon_0 m^*\omega[1+\{(1-\omega_P^2/\omega^2)\omega\tau\}^2], \tag{12}$$

$$\omega_P=\sqrt{ne^2L/m^*\varepsilon_0[1+L(\varepsilon_1'-1)]}, \tag{13}$$

in which ω_P is the resonance plasma frequency that includes plasma depolarization effects via the depolarization factor L introduced in Sec. II, ε_1' is the real part of the dielectric constant before excitation, and n is the concentration of free electrons responsible for plasma effects.

According to Eq. (13), plasma effects depend on the sample shape and are unimportant only for the infinitely long thin strip ($L=0$) when the plasma frequency is zero, and Eqs. (11) and (12) transform to the corresponding equations for free electrons. For a long thin strip of finite length parallel to the electric field the depolarization effects can be reduced but not completely avoided by choosing dimensions to give $\omega_P\ll\omega$. Therefore, plasma depolarization may affect AMTMP measurements, and the transition from plasma to free electron effects can be observed if $\Delta n(t)\gg n_0$ and $\Delta n(t)\approx10^{10}-10^{15}$ cm^{-3}. At this level of excitation the plasma frequency is time dependent also, and this effect will be considered when analyzing experimental data.

C. Trapped electron effects

The harmonic-oscillator model for a trapped electron involves a restoring force proportional to the electron displacement and related to the oscillator binding energy E_b (i.e., a trap depth). The characteristic frequency of the oscillator ω_0 is

$$\omega_0^2=(2/m^*)[(4\pi\varepsilon_0)^2/e^4]E_b^3. \tag{14}$$

The corresponding equations for the changes in the real and imaginary parts of the complex dielectric constant are[22]

$$\delta\varepsilon'_{\rm tr}(t)=\Delta n_{\rm tr}(t)e^2(\omega_0^2-\omega^2)/\varepsilon_0 m^*[(\omega_0^2-\omega^2)^2+(\omega/\tau)^2], \tag{15}$$

$$\delta\varepsilon''_{\rm tr}(t)=\Delta n_{\rm tr}(t)e^2\omega/\varepsilon_0 m^*\tau[(\omega_0^2-\omega^2)^2+(\omega/\tau)^2], \tag{16}$$

in which $\Delta n_{\rm tr}(t)$ is the density of the excess trapped electrons. In contrast to free electrons, trapped electrons make a positive contribution to $\delta\varepsilon'(t)$. When $\omega_0\ll\omega$, Eq. (15) reduces to Eq. (8), which corresponds to the free electron condition. Note that the sign of $\delta\varepsilon'(t)$ changes from positive to negative for a transition from plasma to free electrons, but it changes from negative to positive for a transition from free to trapped electrons. This behavior facilitates interpretation of observed sign changes because each transition occurs at different points as the concentration of excess electrons decreases.

D. Dominant contributions for AMTMP measurements

For $\omega=5.5\times10^{10}$ rad/s, the relative contributions of the various excited species to the complex dielectric constant can be compared using the equations developed above and

$$\delta\varepsilon'=\delta\varepsilon'_{\rm free}+\delta\varepsilon'_{\rm plasm}+\delta\varepsilon'_{\rm trap}, \tag{17}$$

$$\delta\varepsilon''=\delta\varepsilon''_{\rm free}+\delta\varepsilon''_{\rm plasm}+\delta\varepsilon''_{\rm trap}. \tag{18}$$

Because the plasma state occurs only at high carrier density, it will always precede the free electron state, and the only coexisting states will be plasma/trapped electrons and free electrons/trapped electrons. In case of plasma/trapped electrons, their presence cannot be distinguished because each makes a positive contribution to $\delta\varepsilon'(t)$. On the other hand, the negative contribution of free electrons can be distinguished from the positive contribution from the traps having energies within 0.003–0.1 eV. When the mobility is large, free carriers dominate. Trapped electrons dominate when the mobility is small ~0.001 m^2/V s. This analysis is based on the equations presented above using the following ranges of parameters: $\tau=10^{-13}-10^{-15}$ s, $\omega_P=3\times10^9-3\times10^{12}$ Hz (for $\Delta n=10^9-10^{15}$ cm^{-3}), $\omega_0=10^{12}-10^{15}$ Hz (correspond-

ing to the trap depth range 0.001–1 eV). The major contributions to $\delta\varepsilon''(t)$ would be from the free electrons only or from the electron plasma at high concentrations. Because these two states do not coexist, either one or the other will contribute to $\delta\varepsilon''(t)$. These estimations apply at room temperature and will change at sufficiently low temperatures when $\omega\tau \geqslant 1$.

IV. EXPERIMENTAL VALIDATION OF THE HARMONIC-OSCILLATOR MODEL

This section discusses three approaches based on the harmonic-oscillator model in order of increasing complexity based on the number of effects involved. This treatment not only highlights the major features, but also provides quantitative information.

A. Approach I

Transient photoconductivity may include both mobility and carrier concentration changes:

$$\Delta\sigma(t) = n_0 e \Delta\mu(t) + \Delta n(t) e[\mu_0 + \Delta\mu(t)], \tag{19}$$

in which n_0 is the dark (equilibrium) electron concentration, μ_0 is the dark (equilibrium) mobility (only the electron is assumed to contribute due to its larger mobility). Therefore, the relative importance of mobility and electron density changes must be considered in the interpretation of conductivity changes. The results for SI GaAs are used as an example.

Under steady-state illumination, the mobility in SI GaAs increases up to 100% relative to the dark value.[3] A similar increase was observed recently for transient measurements of Hall mobility after pulsed illumination.[10] During much of the time required for the decay of the electron density, the mobility remained almost constant. Since the same period was used for the AMTMP measurement, the mobility was assumed to increase by ~100% after illumination and to stay constant during the decay. Even if the mobility were to change during the decay, it would have a small effect on the kinetic analysis because the excess electron density would be corrected by no more than a factor of ~2.5, which is minor in comparison to the several orders of magnitude change observed during the transient decay. This conclusion is based on a calculation of the electron density using $\mu = 0.73\ \mathrm{m^2/V\,s}$ at 300 K, determined by Hall effect measurements.

A test of this conclusion can be made by comparing the value of $\delta\varepsilon'(t)$ obtained from the frequency change δf_0 [Eq. (4)] with the one calculated from $\delta(\Delta f_{1/2})$ using the following approach. Over the whole range of temperatures (213–358 K) and intensities used for SI GaAs, the change in the real part of the dielectric constant $\delta\varepsilon'(t)$ was negative, indicating that free electrons provided the main contribution to $\delta\varepsilon'(t)$, and plasma effects can be excluded. As a result, only free electrons contribute to $\delta\varepsilon''(t)$. If changes in the mobility are neglected in Eq. (19), $\Delta n(t)$ can be obtained from $\delta(\Delta f_{1/2})$ using Eq. (4) and

$$\delta\sigma = \omega\varepsilon_0\delta\varepsilon''. \tag{20}$$

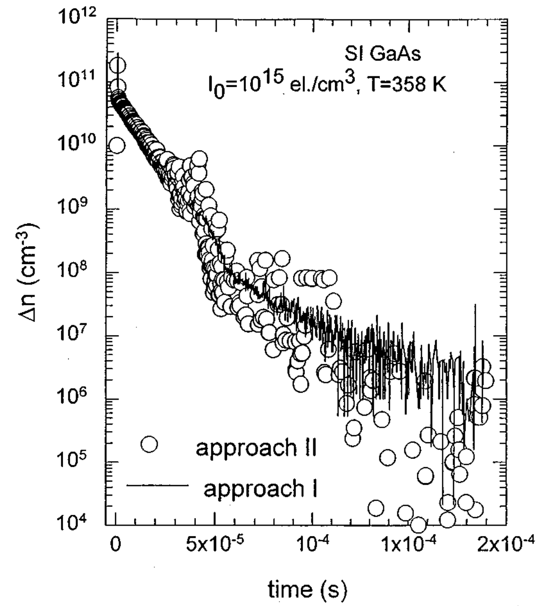

FIG. 2. The decay of the excess electron concentration for SI GaAs (Approaches I and II, see text).

According to Eqs. (8) and (9), both $\delta\varepsilon'(t)$ and $\delta\varepsilon''(t)$ must decay with the same time dependence as $\Delta n(t)$. Values of $\Delta n(t)$ obtained from $\delta(\Delta f_{1/2})$ are given in Fig. 2. Using Eq. (8), these values were used to calculate $\delta\varepsilon'(t)$ (solid line in Fig. 3), which is compared with $\delta\varepsilon'(t)$ (dashed line) determined directly from the frequency shift according to the perturbation theory. The two curves show not only the same time dependence but also they almost coincide numerically. For these calculations, the mobility was adjusted to $1.8\ \mathrm{m^2/V\,s}$ to obtain the best match between the two curves in Fig. 2. These results support the conclusion that mobility changes can be neglected during the decay of the carrier

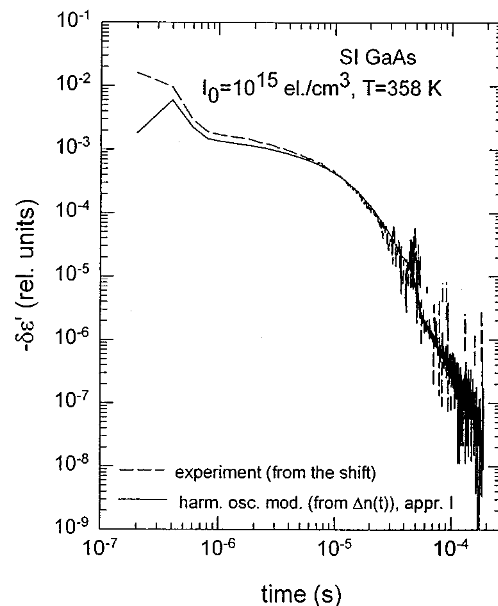

FIG. 3. Time dependence of the change in the real part of the dielectric constant for SI GaAs as obtained from experiment and from the harmonic oscillator model (Approach I).

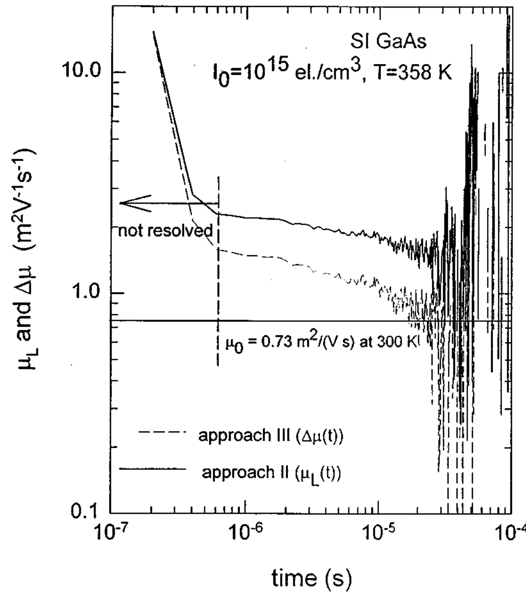

FIG. 4. Time dependence of the light-induced mobility (Approach II) and the mobility changes (Approach III) for SI GaAs. For short times, the time constant of the cavity prevents resolution of the transient.

density. Furthermore, the Drude-Zener theory adequately describes the laser-induced behavior observed for SI GaAs.

For these calculations at 358 K, the SI GaAs sample volume was $5\times1\times0.52$ mm^3. The active volume was defined by the rectangular laser beam (4×1 mm^2), and the absorption coefficient measured at 1064 nm was accurate within 15%. The light intensity corresponded to an initial electron concentration $\sim10^{15}$ cm^{-3}. The sample was treated as an infinitely long, thin strip because the depolarization effects were small (see Sec. II).

B. Approach II

This approach considers the mobility as a time dependent parameter [Eq. (10)]. Exclusion of $\Delta n(t)$ is accomplished by dividing Eq. (8) by Eq. (9) to give the absolute value of the electron mobility after excitation μ_L:

$$\mu_L(t)\equiv\mu_0+\Delta\mu(t)=-\frac{\delta\varepsilon'(t)}{\delta\varepsilon''(t)}\frac{e}{m^*\omega}. \qquad (21)$$

Changes in the real and imaginary parts of the dielectric constant were calculated according to perturbation theory as described in Approach I. The results plotted in Fig. 4 show the mobility stays almost constant from $\sim3\times10^{-7}$ to $\sim4\times10^{-5}$ s at a value ~2 m^2/V s, which is very close to the constant value used in Approach I. These results are consistent with the twofold increase observed for several SI GaAs crystals by the Hall method.[10] Furthermore, the constant region starts at about the same time, but the range cannot be compared because of the noise associated with our technique. The initial apparent fast component is spurious because the corresponding fast components in $\delta\varepsilon'(t)$ and $\delta\varepsilon''(t)$ were not completely resolved. The absolute value of mobility obtained by this method is estimated to be accurate within 50%, which is sufficient to verify the mobility is nearly time independent. Taking into account the time dependence of the mobility, the decay of the concentration of excess electrons is plotted in Fig. 2, which almost coincides with the corresponding curve obtained assuming constant mobility (Approach I).

C. Approach III

This approach, which is the most rigorous treatment, confirms the plasma effect is unimportant for the present measurements. In this case, the finite length of the sample results in a nonzero value of $L=0.007$, which was approximated from Eq. (7). In place of Eqs. (8) and (9), Eq. (11) is divided by Eq. (12):

$$\frac{\delta\varepsilon'(t)}{\delta\varepsilon''(t)}=-\frac{[\mu_0+\Delta\mu(t)]m^*}{e}\,\omega\left(1-\frac{\omega_P^2}{\omega^2}\right). \qquad (22)$$

In this equation, the ratio is not independent of $\Delta n(t)$ because the plasma frequency is concentration dependent. MAPLE V was used to solve Eqs. (19) and (22) for $\Delta\mu(t)$ and $\Delta n(t)$, to get the analytical expression for $\Delta\mu(t)$ (Fig. 4). Comparison of Approaches II and III in Fig. 4 shows that the use of a finite sample length has only a minor effect on the mobility change, and it is essentially constant over the time range where changes can be resolved. Therefore, plasma effects are unimportant over this time range, and the three approaches verify that the conductivity decay for our SI GaAs sample depended on the decay of the excess electron concentration only.

V. TRAPPED ELECTRON CONCENTRATIONS

The presence of shallow traps is well established in SI GaAs,[3,12] although there is some question about the exact density of these traps.[11,33] As discussed above, the positive shift of the resonance frequency indicates free electrons make the dominant contribution to the real part of the dielectric constant, despite the good possibility that shallow traps are filled in SI GaAs after illumination over the time range studied. In contrast, thin-film, polycrystalline CdSe exhibited a negative shift of the frequency, indicating electrons in shallow traps made the dominant contribution to the real part.[13,15] The range of temperatures and times used for SI GaAs was similar to that for CdSe. This difference between CdSe and SI GaAs in regard to $\delta\varepsilon'(t)$ is related to the magnitude of the mobility for each material as discussed below.

Because of the difference in sign of $\delta\varepsilon'(t)$ made by free and trapped electrons, the relative concentrations at which $\delta\varepsilon'(t)=0$ depend on the magnitude of the dark mobility. For CdSe and SI GaAs, the values are 0.0014 and 0.73 m^2/V s, respectively. In the case of SI GaAs, the free electrons dominate at a density of 2×10^{11} cm^{-3} or lower (see Fig. 2), and this value was used to calculate the trapped electron densities at which the contribution of the free electrons to $\delta\varepsilon'(t)$ is a factor of 100 larger than the value due to trapped electrons. Above this trapped electron density, the free electrons begin to lose their domination of $\delta\varepsilon'(t)$. This ratio and Eqs. (8) and (15) were used to calculate $\Delta n_{\rm tr}$ for various binding energies listed in Table I. The characteristic frequencies of the oscillator were calculated according to Eq. (14), and the relaxation time was calculated according to Eq.

TABLE I. Estimated upper limit to trapped electron density. Above this density, the contribution of trapped electrons to $\delta\varepsilon'(t)$ begins to dominate over the one for free electrons. This estimate is based on the free electron densities given in the text.

Trap depth, ΔE (eV)	Concentration of trapped electrons in CdSe (cm^{-3})	Concentration of trapped electrons in SI GaAs (cm^{-3})
0.001	30	1×10^{6}
0.01	2×10^{4}	2×10^{9}
0.1	3×10^{7}	1×10^{12}
0.3	8×10^{8}	4×10^{13}

(10). For CdSe this time was calculated to be 10^{-15} s using $m^*=0.13m_0$. For SI GaAs the following values were used: $m^*=0.063m_0$, $\tau=3.6\times10^{-13}$ s. For a low mobility material like polycrystalline CdSe, it can be seen that density of trapped electrons must be very low before free electrons can dominate $\delta\varepsilon'(t)$. Indeed, the positive change in the real part observed for this material indicates that the actual concentrations of trapped electrons exceeds upper limits given in Table I. On the other hand, for SI GaAs, Table I indicates that 2×10^{11} cm^{-3} free electrons still dominate when the electron density in the 0.1-eV trap is as high as 1×10^{12} cm^{-3}. Consequently, the upper limit for SI GaAs is substantially larger than that for CdSe. It is understood that the ratio chosen is arbitrary; however, these conclusions will not change if a smaller value is chosen. Thus it can be concluded that the effect on $\delta\varepsilon'(t)$ was dominated by free electrons in SI GaAs, but trapped electrons dominated in CdSe because it has a substantially smaller mobility.

This approach sets a more realistic upper limit than the polarizability method[34] used to estimate the trapped electron density in CdSe.[13] Assuming equal polarizability for all traps normally detected by photodielectric effect (in the energy range 0.003–0.3 eV), the concentration of electrons in shallow traps after illumination was estimated to be less than 10^{11} cm^{-3} in SI GaAs, which is substantially lower than the sum of the values in Table I. This approach suffers from the assumption that all traps within the 0.003–0.3-eV range have the same polarizability. Because this condition applies only to a few tens of meV depth for the hydrogenlike center, the concentration of electrons in traps deeper than 10–20 meV was underestimated. In fact, semiempirical calculations from polarizability measurements (i.e., second-order Stark effect) made for AgCl showed that polarizability of electrons in hydrogenlike states was about one order of magnitude bigger than the value for free electrons and about four orders of magnitude bigger than that for deep traps.

VI. CONCLUSIONS

General second cavity perturbation expressions have been derived for the changes in the complex dielectric constant without simplifying assumptions. By introducing the depolarization factor L into these general expressions, it is possible to generate simplified expressions obtained by others for appropriate sample geometries. As a result, changes in the complex dielectric constant can be treated in a unified way. The implications of the harmonic-oscillator theory for AMTMP measurements were analyzed in terms of the distinctive behavior of free and bound electrons. The model was applied to several basic electron states: free, shallowly trapped, deeply trapped, plasma. The relative contribution of these states to changes in the complex dielectric constant depends on the total concentration of the carriers. The harmonic-oscillator model was found to be consistent with the experimental results obtained for SI GaAs for which the dominant contribution to the changes in the real part of the complex dielectric constant came from the free (conduction band) electrons. The different behavior of CdSe and SI GaAs in regard to the real part of the dielectric constant could be ascribed to the large difference in their mobility values.

ACKNOWLEDGMENTS

This work was supported in part by a grant from the Natural Sciences and Engineering Research Council of Canada to M.C.

[1] R. H. Bube, J. Appl. Phys. **31**, 315 (1960).
[2] B. R. Holeman and C. Hilsum, J. Phys. Chem. Solids **22**, 19 (1961).
[3] R. H. Bube and H. E. MacDonald, Phys. Rev. **128**, 2062 (1962); **128**, 2071 (1962).
[4] T. Kinsel and I. Kudman, Solid-State Electron. **8**, 797 (1965).
[5] S. S. Li and C. I. Huang, J. Appl. Phys. **43**, 1757 (1972).
[6] A. L. Lin, E. Omelianovski, and R. H. Bube, J. Appl. Phys. **47**, 1852 (1976).
[7] R. E. Kremer, M. C. Arikan, J. C. Abele, and J. S. Blakemore, J. Appl. Phys. **62**, 2424 (1987); **62**, 2432 (1987).
[8] M. S. Wang and J. M. Borrego, J. Electrochem. Soc. **137**, 3648 (1990).
[9] P. K. Giri and Y. N. Mohapatra, J. Appl. Phys. **78**, 262 (1995).
[10] V. Kazukauskas, J. Storasta, and J.-V. Vaitkus, J. Appl. Phys. **80**, 2269 (1996).
[11] G. M. Martin, J. P. Farges, G. Jacob, J. P. Hallais, and G. Poiblaud, J. Appl. Phys. **51**, 2840 (1980).
[12] M. R. Burd and R. Braunstein, J. Phys. Chem. Solids **49**, 731 (1988).
[13] S. Yu. Grabtchak and M. Cocivera, Phys. Rev. B **50**, 18 219 (1994).

[14] S. Grabtchak and M. Cocivera, Prog. Surf. Sci. **50**, 305 (1995).
[15] S. Yu. Grabtchak and M. Cocivera, J. Appl. Phys. **79**, 786 (1996).
[16] S. Grabtchak and M. Cocivera, *Proceedings of the Symposium on Diagnostic Techniques for Semiconductor Materials* (The Electrochemical Society, Montreal, 1997), Vol. 97-12, pp. 235–242.
[17] S. Grabtchak and M. Cocivera, *Proceedings of the Symposium on Electrically Based Microstructural Characterization II* (MRS, Pittsburgh, in press).
[18] J. C. Slater, Rev. Mod. Phys. **18**, 441 (1946).
[19] H. M. Altshuller, in *Handbook of Microwave Measurements*, edited by M. Suchner and J. Fox (Interscience, New York, 1963), Vol. 2, Chap. 9.
[20] J. P. Spoonhower and R. J. Deri, J. Imaging Sci. **31**, 141 (1987).
[21] W. H. Hartwig and J. J. Hinds, J. Appl. Phys. **40**, 2020 (1969).
[22] J. J. Hinds and W. H. Hartwig, J. Appl. Phys. **42**, 170 (1971).
[23] L. J. Buravov and I. F. Shchegolev, Prib. Tehk. Eksp. **2**, 171 (1971).
[24] S. K. Khanna, E. Ehrenfreund, A. F. Garito, and A. J. Heeger, Phys. Rev. B **10**, 2205 (1974).
[25] B. Lehndorff, Meas. Sci. Technol. **3**, 822 (1992).
[26] R. Hutcheon, M. de Jong, and F. Adams, J. Microwave Power Electromagn. Energy **27**, 87 (1992).
[27] L. D. Landau and E. M. Lifshitz, *Electrodynamics of Continuous Media*, 2nd ed. (Pergamon, New York, 1984).
[28] C. Kittel, *Introduction to Solid State Physics*, 5th ed. (Wiley, New York, 1976).
[29] J. A. Osborn, Phys. Rev. **67**, 351 (1945).
[30] G. Dresselhaus, A. F. Kip, and C. Kittel, Phys. Rev. **100**, 618 (1955).
[31] T. S. Benedict and W. Shockley, Phys. Rev. **89**, 1152 (1953).
[32] E. N. Glezer, Y. Siegel, L. Huang, and E. Mazur, Phys. Rev. B **51**, 6959 (1995).
[33] M. L. Sadowski and M. Grynberg, J. Phys. Chem. Solids **56**, 619 (1995).
[34] R. J. Deri and J. P. Spoonhower, Phys. Rev. B **25**, 2821 (1982).